The role of high cycle fatigue (HCF) onset in Francis runner reliability

M Gagnon[1], S A Tahan[1], P Bocher[1] and D Thibault[2]

[1] École de technologie supérieure (ÉTS), 1100, Notre-Dame Street West, Montréal, QC, H3C 1K3, Canada
[2] Institut de recherche d'Hydro-Québec (IREQ), 1800 Lionel-Boulet, Varennes, QC, J3X 1S1, Canada

E-mail: martin.gagnon.8@ens.etsmtl.ca

Abstract. High Cycle Fatigue (HCF) plays an important role in Francis runner reliability. This paper presents a model in which reliability is defined as the probability of not exceeding a threshold above which HCF contributes to crack propagation. In the context of combined Low Cycle Fatigue (LCF) and HCF loading, the Kitagawa diagram is used as the limit state threshold for reliability. The reliability problem is solved using First-Order Reliability Methods (FORM). A study case is proposed using in situ measured strains and operational data. All the parameters of the reliability problem are based either on observed data or on typical design specifications. From the results obtained, we observed that the uncertainty around the defect size and the HCF stress range play an important role in reliability. At the same time, we observed that expected values for the LCF stress range and the number of LCF cycles have a significant influence on life assessment, but the uncertainty around these values could be neglected in the reliability assessment.

1. Introduction

Our capacity to select relevant models for reliability assessment of structural components depends mostly on available data and knowledge at the time of the study. We observe in structures, such as large Francis hydroelectric turbine runners, where the cost of downtime is high and *in situ* inspection methods are limited, that cracks often reach a detectable size only after the onset of High Cycle Fatigue (HCF). Furthermore, because large Francis runners can sustain significant damage without incurring any safety issues, the main concerns are repair cost and downtime. Hence, a crack must be repaired as soon as possible in order to minimize the cost of repair, and concurrently, the time between inspections must be maximized to reduce downtime. This leads to the following dilemma: if the HCF onset has occurred, a longer time between inspections leads to longer cracks to be repaired, and, at the same time, if the component is inspected before the HCF onset, we incur downtime and maintenance costs with limited information on the state of the structure because the detectable flaw size has not been reached. Therefore, we propose to move away from the typical fatigue limits, as commonly seen in SN curves and critical crack lengths, which do not adequately reflect this reality, in favor of a limit state directly related to the HCF onset [1].

In this study, we state that the HCF onset should be used as the proper limit state for reliability assessment. This statement relies on two basic assumptions:

- After HCF onset, significant crack growth will be induced and the crack length will therefore be linked to the time of operation rather than being a function of the number of low cycle fatigue (LCF) cycles.
- If significant growth is expected, a crack needs to be repaired as soon as possible in order to minimize costs.

The HCF effect on crack growth is presented in Figure 1b. In this figure, we observe the crack propagation from the strains measured on a Francis runner shown in Figure 1a. The crack growth simulations show that slow crack growth can be expected when minimal time at maximum opening is accounted for (LCF only). However, during normal operation, almost 24 hours of operation at maximum opening can be expected (LCF+HCF). In this case, we reach a point (HCF onset) after which crack growth speed increases exponentially. The goal of the study is to understand the role of the HCF onset, as observed in Figure 1b, on the reliability of a Francis runner using probabilistic methods and parameter values representative of observed data.

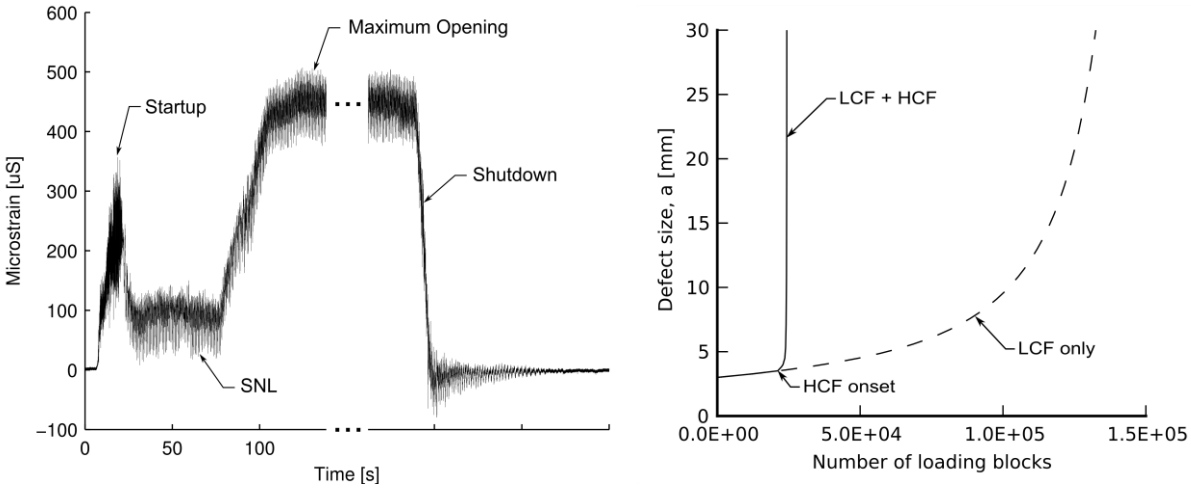

Figure 1. (a) Example of loading measured on a large Francis runner (b) Crack propagation results

The thresholds below which the HCF loading does not contribute to crack propagation can be presented using the Kitagawa diagram. This diagram, developed by Kitagawa and Takahashi [2], is drawn using two thresholds: the threshold for fatigue crack growth as defined in the framework of Linear Elastic Fracture Mechanics (LEFM), and the fatigue limit for a given number of cycles which usually correspond to 1E+07 cycles for materials exhibiting an endurance limit. It should be noted that this diagram can also be extended to include more parameters, such as notch effects [3] and multi-axial criteria [4]. In this paper, we intend to use the limits formed by the Kitagawa diagram combined with the El Haddad correction factor [5], which account for short crack behaviours, to assess the reliability of large Francis turbine runners.

The paper is structured as follows: first, the HCF onset reliability is defined, followed by the methodology used to solve the proposed reliability problem. Next, a study case is proposed from which reliability results are obtained using typical design specifications and observed *in situ* data. Finally, the paper concludes with a discussion on the importance of each parameter in the design, maintenance and operation of the Francis runner.

2. High cycle fatigue (HCF) onset reliability

To assess the fatigue reliability of a structure, we need the following elements: a properly defined limit state model, a reliability criterion and characterized uncertainty sources. In this study, the limit state is defined as the thresholds proposed by Kitagawa and Takahashi [2], combined with the correction factor developed by El Haddad et al. [5]. In this limit state, the El Haddad et al. [5] correction factor accounts for short crack growth by asymptotically matching the LEFM threshold and the fatigue limit.

This limit state, commonly called the Kitagawa diagram, is shown in Figure 2a, and the uncertainties associated with the parameters of the reliability problem are shown in Figure 2b.

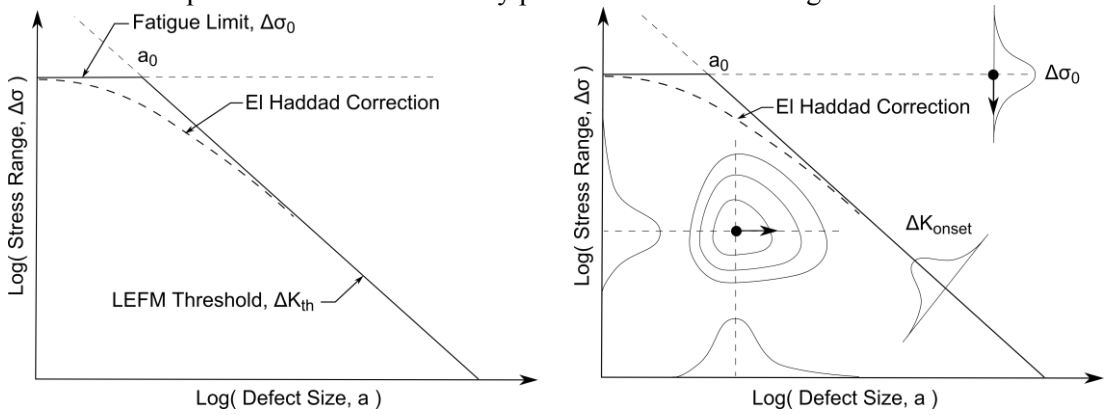

Figure 2. (a) Schematic Kitagawa diagram, (b) Schematic probabilistic Kitagawa diagram

In the Kitagawa diagram, the limit formed by the LEFM threshold is obtained from the stress intensity factor solution defined as follows:

$$\Delta K = \Delta\sigma\sqrt{\pi a}\, Y(a) \tag{1}$$

where ΔK is the stress intensity factor, $\Delta\sigma$ is the stress cycle range, a is the crack length and $Y(a)$ is the stress intensity correction factor for a given geometry. The limit state equation is obtained by replacing ΔK by the LEFM threshold ΔK_{th} in Eq. (1), which is rewritten as follows:

$$\Delta\sigma_{th} = \frac{\Delta K_{th}}{\sqrt{\pi a}\, Y(a)} \tag{2}$$

To capture short crack growth, El Haddad et al. [5] proposed to asymptotically match the limits defined by LEFM and the fatigue limit $\Delta\sigma_0$ using the reference crack length a_0 as a correction factor. The correction factor a_0 is added to the crack length a in Eq. (2) to obtain:

$$\Delta\sigma_{th} = \frac{\Delta K_{th}}{\sqrt{\pi(a+a_0)}\, Y(a+a_0)} \tag{3}$$

where the constant a_0 represents the transition between both limits, and is obtained by solving the following equation:

$$a_0 = \frac{1}{\pi}\left(\frac{\Delta K_{th}}{\Delta\sigma_0\, Y(a_0)}\right)^2 \tag{4}$$

For infinite life, $\Delta\sigma_0$ is the endurance limit. However, in some cases, the limit state for a finite number of cycles N might also be of interest either because the number of cycles for infinite life might not have been reached in a given time interval or because the material has no endurance limit. In those instances, a finite number of stress cycles N can be accounted for using the fatigue limit at N cycles rather than the endurance limit. This approach is similar to the model developed by Ciavarella and Monno [6]. Furthermore, it is relevant to note that all the parameters in Eq. (3) and Eq. (4) can be considered as independent random variables.

Now that the limit state has been specified, a criterion for failure must be defined. This criterion is expressed as follows:

$$g(x) \le 0 \tag{5}$$

with a probability of failure:

$$P_f = \int_{g(x)\leq 0} f_X(x)\, dx \tag{6}$$

and reliability:

$$R = 1 - P_f \tag{7}$$

in which, x is an n-dimensional vector of random variables with a joint density function $f_X(x)$. If we define the failure as the HCF onset, then $g(x)$ becomes:

$$g(a, \Delta\sigma) = \Delta\sigma - \frac{\Delta K_{onset}}{\sqrt{\pi(a+a_0)}\, Y(a+a_0)} \tag{8}$$

In our study, we have chosen to consider four uncertainty sources: the defect size a, the LCF stress range $\Delta\sigma_{LCF}$, the HCF stress range $\Delta\sigma_{HCF}$ and the number of LCF cycles. For each of these variables, the uncertainty and expected value must be characterized using a proper distribution type, location and scale.

3. FORM/SORM approximation

Two numerical approaches can be used to solve the probability of HCF onset defined by Eq. (6) in the previous section. The approaches can either be simulation-based, such as the Monte Carlo (MC) simulation and its variants, or analytical, using approximations like the First-Order Reliability Method (FORM) and the Second-Order Reliability Method (SORM). An advantage of the simulation-based method, such as crude MC, is that it asymptotically converges to the exact values for a number of simulations $N \to \infty$ but nevertheless has a drawback, common to all simulation-based methods, of possibly requiring a prohibitive number of simulations in order to provide reliable results for a low-probability estimate. On the other hand, analytical methods are based on the approximation of the probability of failure leading to a minimal numerical burden in exchange for accuracy.

The FORM/SORM approximation relies on the assumption that a transformation in the form $\underline{U} = T(\underline{X})$ exists, mapping the physical space to a standard space. The transformation is expressed as follows:

$$P_f = \int_{g(\underline{X})\leq 0} f(\underline{x})\, d\underline{x} = \int_{g(T(\underline{X}))\leq 0} \varphi(\underline{u})\, d\underline{u} \tag{9}$$

where $\varphi(\underline{u})$ is an n-dimensional standard normal density with independent components.

Several such transformation methods are available. The Rosenblatt transform [7] was chosen in this study because of its flexibility, which allows the dependency structures between random variables to be modeled using the copula theory. The Rosenblatt transform is defined as follows:

$$\underline{U} = T(\underline{X}) = T_2(\underline{X}) \circ T_1(\underline{X}) \tag{10}$$

$$\begin{aligned} T_1 :&\quad \Re^n \to \Re^n \\ \underline{X} \mapsto \underline{Y} &= \begin{pmatrix} F_1(X_1) \\ F_2(X_2 \mid X_1) \\ F_3(X_3 \mid X_1, X_2) \\ \vdots \\ F_n(X_n \mid X_1, X_2, \ldots, X_n) \end{pmatrix} \end{aligned} \tag{11}$$

$$T_2: \quad \Re^n \to \Re^n$$
$$\underline{Y} \mapsto \underline{U} = \begin{pmatrix} \Phi^{-1}(Y_1) \\ \Phi^{-1}(Y_2) \\ \vdots \\ \Phi^{-1}(Y_n) \end{pmatrix} \tag{12}$$

where $\underline{X}$ in $\Re^n$ is a continuous random vector defined by its marginal cumulative distributions F_i and copula. It should be noted that the conditioning order in Eq. (11) will influence the shape limit state in the standard space $\underline{U}$ and the results of the FORM/SORM approximation. Because the stress range $\Delta\sigma$ is considered independent of the defect size a, the assumption can be made that the random vector $\underline{X}$ has an independent copula and, with such an assumption, the Rosenblatt transform in Eq. (10) becomes:

$$\underline{U} = \begin{pmatrix} \Phi^{-1}(F_1(X_1)) \\ \Phi^{-1}(F_2(X_2)) \\ \vdots \\ \Phi^{-1}(F_n(X_n)) \end{pmatrix} \tag{13}$$

In the standard space $\underline{U}$, the probability of failure P_f can be obtained with a linear approximation (FORM) or a quadratic approximation (SORM), as shown in Figure 3. In this space $\underline{U}$, the Most Probable Point (MPP) of failure, also named the design point u^*, is located at the shortest distance between the origin and the limit state $g(\underline{U}) = 0$. The distance to the MPP is called the Hasofer-Lind reliability index β_{HL}.

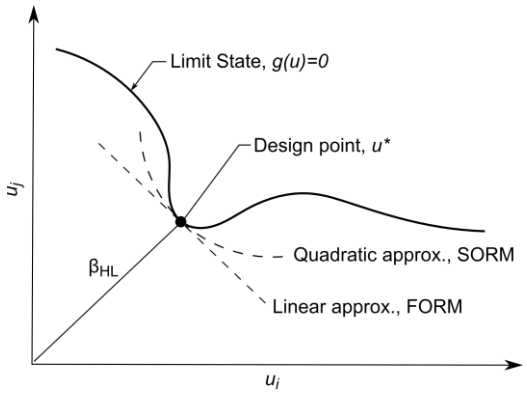

Figure 3. Schematic isoprobabilist space

The FORM approximation of the probability of failure P_f can be calculated directly from the Hasofer-Lind index β_{HL} and is given by:

$$P_f = 1 - \Phi(\beta_{HL}) = \Phi(-\beta_{HL}) \tag{14}$$

where $\beta_{HL} = \left\| \underline{u}^* \right\|$ is the standard normal cumulative function and $\underline{u}^* = \min \left\| \underline{u} \right\|$ for $g(\underline{U}) \le 0$. The main numerical burden of this approximation resides in finding the location of the design point $\underline{u}^*$. Note that the results obtained with the FORM approximation are only accurate when the limit state is linear in the standard space $\underline{U}$. Likewise, results from the SORM approximations are only accurate when the limit state at the design point is close to quadratic in the standard space $\underline{U}$. In this study, the accuracy

of the FORM approximation will be considered sufficient for our application. We refer the reader to the work of Rackwitz [8] and the work of Ditlevsen and Madsen [9] for a complete overview of the theory and the methods used in structural reliability analysis.

4. Study case

We have chosen to use the data observed on a Francis runner from a hydroelectric plant in Quebec, Canada, for our study case. The facility was chosen because *in situ* measurements combined with historical operational data were available. In our study case, we consider the following parameters as random: the defect size a, the LCF stress range $\Delta\sigma_{LCF}$, the HCF stress range $\Delta\sigma_{HCF}$ and the number of LCF cycles N_{LCF}. For each of these random parameters, the distribution type with its location and scale is defined with regards to the available data.

The critical location studied is a cutout near the runner crown on each blade. During the *in situ* strain measurements, the Francis runner was instrumented with strain gauges at this particular location. The position of the strain gauge is shown in Figure 4.

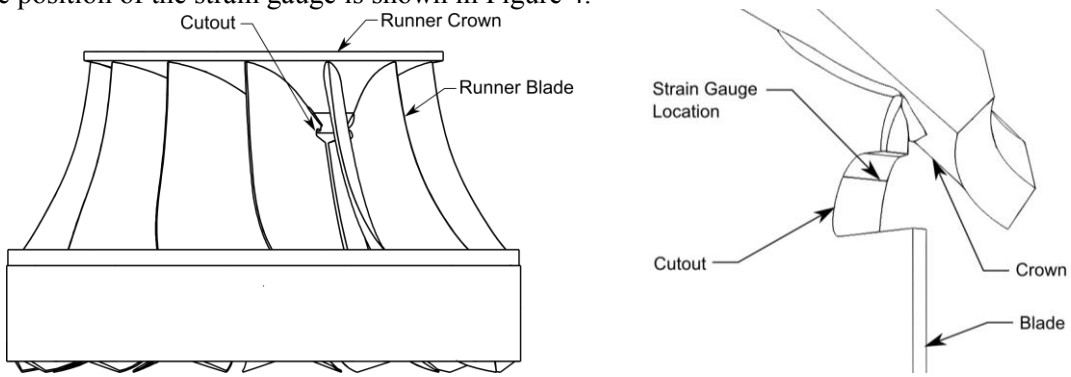

Figure 4. Francis runner diagram. (a) Overall view of the runner, (b) Detailed view of the measured location

The flaw geometries generally expected are either surface flaws or embedded flaws, as shown in Figure 5a. However, in our particular case, the critical zone is near the corner of the blade section in the cutout region. As a result, the corner flaw geometry is more representative of our geometry, as shown in Figures 5b and 5c. In this paper, however, only the corner flaw in Figure 5c is studied in order to limit the number of random parameters considered. For this defect geometry, both the stress intensity correction factor $Y(a)$ and the crack growth are calculated according to the British Standard BS7910 [9]. In the study case, the expected initial defect size a is defined as 1.5 mm for illustrative purposes.

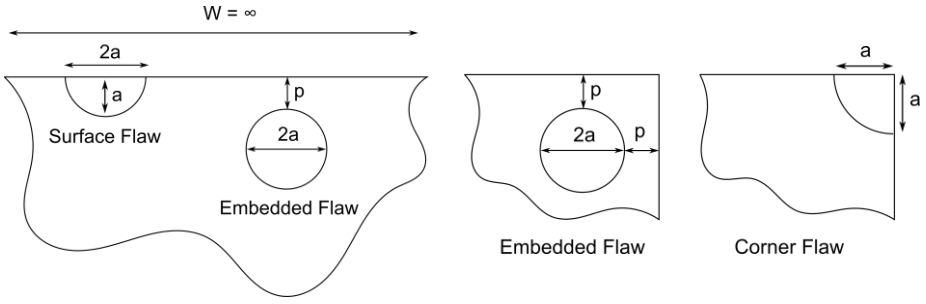

Figure 5. Flaw geometries. (a) Typical surface and embedded flaw, (b) Corner embedded flaw, (c) Corner flaw

Note that, in our study case, the loading is simplified to two stress ranges: an LCF stress range $\Delta\sigma_{LCF}$ and an HCF stress range $\Delta\sigma_{HCF}$, as shown in Figure 6. Such a representation is similar to the

strain measured during a typical loading sequence (Figure 1a) if we neglect the startup and shutdown phases of the loading sequence. Even while these transients are not considered in this study, it should be noted that the amplitude of the startup transients can have a significant influence on life expectancy, and are directly related to the control scheme used [11, 12]. In our simplified loading, we defined the mean LCF stress range $\Delta\sigma_{LCF}$ as 100 MPa and the mean HCF stress range $\Delta\sigma_{HCF}$ as 20 MPa. These expected values are representative of the strain range observed during the *in situ* measurements at the cutout location; however, the distribution type and scale of both the LCF stress range $\Delta\sigma_{LCF}$ and HCF stress range $\Delta\sigma_{HCF}$ were chosen arbitrarily for illustrative purposes. Nonetheless, the values are considered representative of observed values even if they may not have been validated using experimental data.

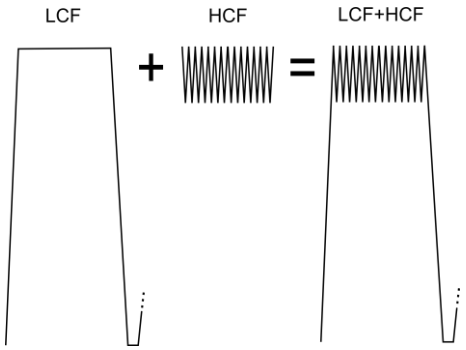

Figure 6. Schematic example of combined LCF+HCF loading

Using the 5 years of historical operational data available for this runner, the number of LCF cycles N_{LCF} was extrapolated over a 100-year period, using semi-Markov simulations [13]. The expected value and uncertainty of the number of LCF cycles N_{LCF} were estimated using 400 semi-Markov simulations, and the results from these simulations are shown in Figure 7a. In this figure, we observe that the results include both the typical design specification of 1/day and the results from the available observed data replicated over the 100-year period. In our reliability assessment, the probability distribution observed after 100 years was used to obtain the distribution parameters for the number of LCF cycles N_{LCF} as shown in Figure 7b.

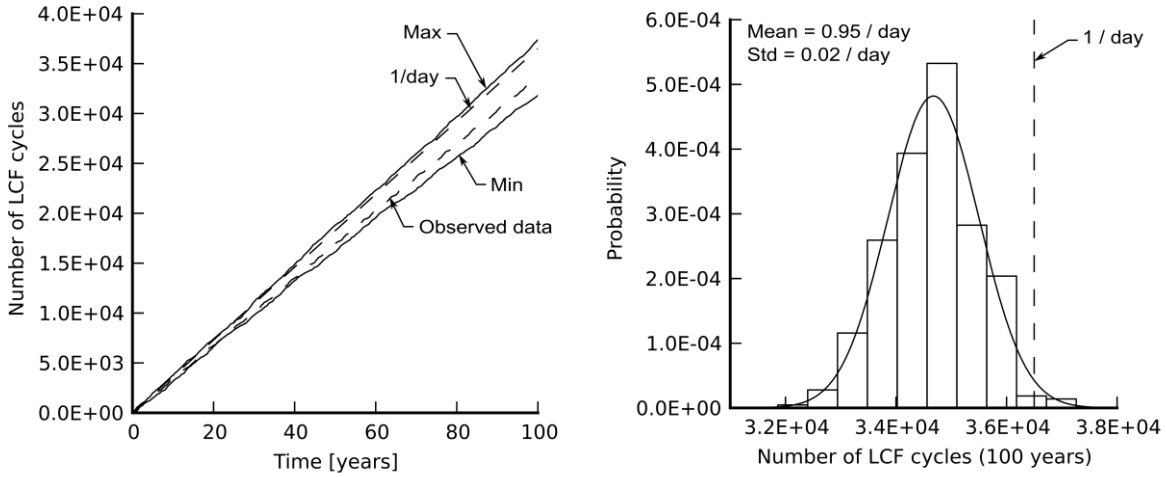

Figure 7. Extrapolated LCF cycles. (a) Cumulative number of LCF cycles, (b) Probability distribution of LCF

The model parameters used for the study case are summarized in Table 1. Note that both the LEFM threshold ΔK_{th} and the endurance limit $\Delta\sigma_0(N=10^7)$ are considered deterministic parameters in this study.

Table 1. Study case parameters

	Location	Scale	Distribution	Units
ΔK_{th}	2.0	-	-	MPa $m^{1/2}$
$\Delta\sigma_0(N=10^7)$	85.6	-	-	MPa
a	1.5	0.5	Gumbel	mm
σ_{LCF}	100.0	10.0	Normal	MPa
σ_{HCF}	20.0	1.0	Gumbel	MPa
N_{LCF}	0.95	0.02	Normal	day^{-1}

5. Results / discussion

The results of four operation scenarios are shown in Figure 8. The first scenario is N_{LCF} = 0.95/day, which uses the parameters in Table 1. The other three scenarios are: N_{LCF} = 0.5/day, N_{LCF} = 1/day and N_{LCF} = 2/day, in which N_{LCF} is considered deterministic. We observe that a small change in the number of LCF cycles N_{LCF} can have a large influence on the life expectancy for a given probability of failure P_f = 1/1000. This is the consequence of the slow rate of crack propagation generated by the LCF cycles. For a probability of failure P_f = 1/1000, the life expectancy goes from 40 years at N_{LCF} = 2/day to what could be considered an infinite life given typical design requirements at N_{LCF} = 0.5/day, for which a life expectancy of 160 years is obtained.

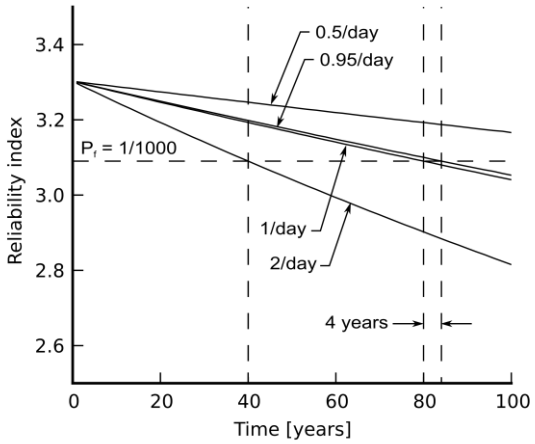

Figure 8. Reliability Index vs. Time for various operation scenarios

In the design specifications, a life expectancy of 60 years is often used, and detailed results for 60 years of operation are presented in Table 2. The probability of failure obtained might look small, but if we consider that these results represent the probability for only one runner blade, the overall probability of a runner having no cracked blade can be approximated by:

$$R = (1 - P_f)^n \tag{15}$$

in which n is the number of blades of the runner. We observe that, for a 13 blades runner such as the one in our study, the reliability is significantly lower than that expected from the probability of failure P_f obtained at a specific location on one runner blade. If we look at the perspective of a facility

composed of many identical runners, even a small probability of failure might have a significant impact on expected maintenance costs.

Table 2. Detailed results for 60 years of operation for a given location

	0.5/day	1/day	2/day
Physical space design point, x^* $[\, a, \sigma_{HCF}, N_{LCF}, \sigma_{LCF} \,]$	[4.6, 22.5, 0.5, 101.0]	[4.5, 22.4, 1.0, 101.4]	[4.4, 22.1, 2.0, 102.5]
Standard space design point, u^* $[\, a, \sigma_{HCF}, N_{LCF}, \sigma_{LCF} \,]$	[2.9, 1.4, 0.0, 0.1]	[2.8, 1.3, 0.0, 0.1]	[2.7, 1.2, 0.0, 0.3]
Hasofer-Lind reliability index, β_{HL}	3.22	3.14	2.98
FORM probability, P_f	0.643 E -3	0.853 E -3	1.427 E -3
Runner reliability, $(1-P_f)^{13}$	0.991	0.989	0.981

Furthermore, we would like to note that for each random variable, the uncertainty does not have the same influence on the probability of exceeding the HCF onset threshold. The influence of a random variable uncertainty can be calculated as follows:

$$\alpha_i^2 = \frac{(u_i^*)^2}{\beta_{HL}{}^2} \tag{16}$$

in which α_i^2 is the importance factor of the uncertainty around a given random parameter. The importance factors α_i^2 for 1 year and 60 years of operation using the parameters in Table 1 are shown in Figure 9. Note that the importance factors α_i^2 do not change significantly between Figures 9a and 9b. Furthermore, we observe that the uncertainty around the defect size a has the most influence, followed by the uncertainty around the HCF stress range $\Delta\sigma_{HCF}$ and that the influence of the other random variables uncertainty is negligible. In our case, the uncertainty around the number of LCF cycles N_{LCF} and the LCF stress range $\Delta\sigma_{LCF}$ have no influence on the Hasofer-Lind reliability index β_{HL}, which means that both variables could have been considered deterministic. Hence, no assumption needs to be made about expected distribution and uncertainties for these parameters. However, due to the sensitivity of life expectancy to these parameters, care should be taken in the choice of expected values

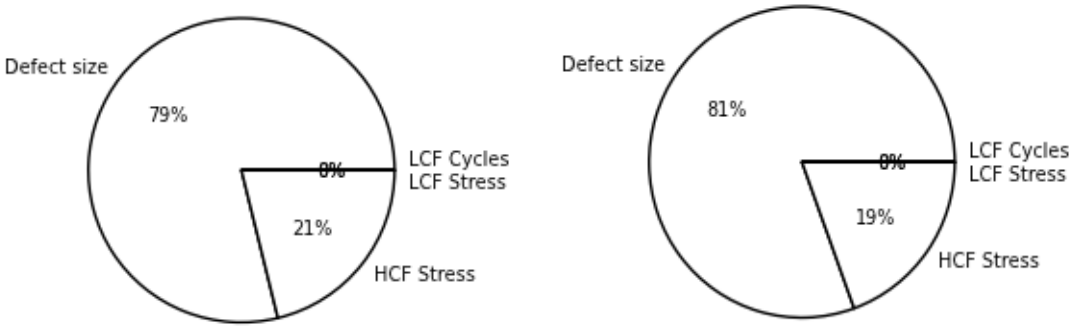

Figure 9. Uncertainties importance Factor for 0.95/day LCF cycles. (a) 1 year, (b) 60 years

Moreover, the two variables for which uncertainty has the highest importance are mostly controlled by the manufacturer, meaning that the utility often relies on data from inspections made during manufacturing, and on stress levels calculated during design, for reliability assessment. The results obtained in this study highlight the need for more collaboration between the manufacturer and the

utility in order to reduce uncertainties around both the defect size a and HCF stress range $\Delta\sigma_{HCF}$. We believe that, in order to reduce defect size uncertainty, the inspections performed during manufacturing and the inspections performed after commissioning must be combined and optimized. Further, we believe that *in situ* field measurement could play a significant role in the reduction of stress level uncertainties and the validation of calculated design values, leading to improved reliability.

6. Conclusions

The goal of this paper was to obtain more insight into the role of HCF onset in the reliability of the Francis runner. The HCF onset was defined as the point in time after which a previously undetected or uncritical defect will rapidly reach detectable size. Assuming that such defect needs to be repaired as soon as detected, the limit state for reliability assessments has been defined as the probability of reaching the HCF onset. Using FORM approximations to solve the reliability problem, we have observed the following:

- Reliability results are sensitive to expected LCF stress range $\Delta\sigma_{LCF}$ and number of cycles N_{LCF} but not to their uncertainties.
- Defect size a uncertainty has the highest importance factor, meaning that reliability results are more sensitive to the uncertainties around this parameter.
- HCF stress range $\Delta\sigma_{HCF}$ uncertainty has a significant influence on reliability, which, as for defect size a, means that results are sensitive to the uncertainties around this parameter.

These observations highlight the need for a better understanding and optimization of the runner inspections in order to define proper defect size a expected value and uncertainty. Furthermore, due to the importance of the uncertainty around the HCF stress range $\Delta\sigma_{HCF}$, we believe that *in situ* measurements should play a more important role in the validation of design calculation and evaluation of uncertainty levels. We also observe that the rate at which reliability decreases depends on the expected values of the LCF parameters, for which uncertainty do not influence the reliability results. However, the sensitivity to these expected values leads to a need for well-defined methodologies to define safe expected levels. Finally, we would like to mention that the structural reliability methods used in this study are well developed in the literature [8, 9], and it is in the authors' opinion that such methods should play an important role in the understanding of probability crack detection in hydroelectric Francis runners and, potentially, in any structures subjected to combined HCF-LCF loading.

Acknowledgments

The authors would like to thank the Institut de recherche d'Hydro-Québec (IREQ), Andritz Hydro Ltd, the National Sciences and Engineering Research Council of Canadian (NSERC) and the École de technologie supérieure (ÉTS) for their support and financial contribution.

Nomenclature

a	Crack length [mm]	W	Section width [mm]
a_0	El. Haddad et al. [4] correction factor [mm]	$Y(\cdot)$	Stress intensity correction factor
$f(\cdot)$	Joint density function	x	Multi-dimensional random vector variables
F_i	Marginal cumulative probability distribution	x^*	Physical space design point
$g(\cdot)$	Failure criteria	X	Physical space
p	Distance from surface [mm]	α_i^2	Importance factor
P_f	Probability of failure	β_{HL}	Hasofer-Lind Reliability index
n	Number of blades	ΔK	Stress intensity factor [MPa m^{-1}]

N	Number of stress cycles	ΔK_{th}	LEFM crack growth threshold [MPa m^{-1}]
N_{LCF}	Number of LCF stress cycles	$\Delta\sigma$	Stress cycle range [MPa]
R	Reliability	$\Delta\sigma_{HCF}$	HCF stress cycle range [MPa]
$T(\cdot)$	Transformation	$\Delta\sigma_{LCF}$	LCF stress cycle range [MPa]
u	Multi-dimensional random vector variables	$\Delta\sigma_{th}$	Threshold Stress cycle range [MPa]
u^*	Standard space design point	$\Delta\sigma_0$	Fatigue limit [MPa]
U	Standard space	$\varphi(\cdot)$	Standard normal probability density

References

[1] Gagnon M, Tahan A, Bocher P and Thibault D 2012 A probabilistic model for the onset of High Cycle Fatigue (HCF) crack propagation: application to hydroelectric turbine runner (To be published)
[2] Kitagawa H and Takahashi S 1976 Applicability of fracture mechanics to very small cracks in: ASM *Proceedings of 2nd International Conference on Mechanical Behaviour of Materials Metalspark (Ohio, USA, 1976)* pp 627-631
[3] Atzori B and Lazzarin P 2002 *International Journal of Fracture* **118** 271-284.
[4] Thieulot-Laure E, Pommier S and Fréchinet S 2007 *International J. of Fatigue* **29** 1996-2004
[5] El Haddad M H, Topper T H and Smith K N 1979 *Engineering Fracture Mechanics* **11** 573-584
[6] Ciavarella M and Monno F 2006 *International Journal of Fatigue* **28** 1826-1837
[7] Lebrun R and Dutfoy A 2009 *Probabilistic Engineering Mechanics* **24** 577-584
[8] Rackwitz R 2011 *Structural Safety* **23** 365-395.
[9] Ditlevsen O and Madsen H O 2007 *Structural Reliability Methods* (Internet edition 2.2.7)
[10] British Standards Institute 2005 *Guidance on Some Methods for the Assessment of Flaws in Welded Construction* (UK:British: Standards Institute) BS7910:2005.
[11] Gagnon M, Tahan A, Bocher P and Thibault D 2010 expectancy *IOP Conference Series: Earth and Environmental Science* **12** 012107
[12] Gagnon M, Tahan A, Bocher P and Thibault D 2012 *Mechanical Systems and Signal Processing* doi:10.1016/j.ymssp.2012.02.006.
[13] Szczota M, Gagnon M, Tahan A, Marcouiller L and Thibault D 2011 *Modeling Operation History of Hydroelectric Turbines Hydrovision 2011* Sacramento California USA